

15

GRB Cosmology

VOLKER BROMM¹ and ABRAHAM LOEB²*(1) Astronomy Department, The University of Texas at Austin, USA**(2) Astronomy Department, Harvard University, Cambridge, USA***Abstract**

Current observations are about to open up a direct window into the final frontier of cosmology: the first billion years in cosmic history when the first stars and galaxies formed. Even before the launch of the *James Webb Space Telescope*, it might be possible to utilize Gamma-ray Bursts (GRBs) as unique probes of cosmic star formation and the state of the intergalactic medium (IGM) up to redshifts of several tens, when the first (Population III) stars had formed. The *Swift* mission, or future satellites such as EXIST, might be the first observatories to detect individual Population III stars, provided that massive metal-free stars were able to trigger GRBs. Spectroscopic follow-up observations of the GRB afterglow emission would allow to probe the ionization state and metal enrichment of the IGM as a function of redshift.

15.1 Introduction

One of the important goals in modern cosmology is to understand how the first stars formed at the end of the cosmic dark ages, and how they transformed the initially simple, homogeneous universe into a state of ever increasing complexity (e.g., Barkana & Loeb 2001; Miralda-Escudé 2003; Bromm & Larson 2004; Ciardi & Ferrara 2005; Loeb 2006). The first stars [so-called Population III (Pop III)] are predicted, based on results from numerical simulations, to have started forming at redshifts $z > 20$, and to have been predominantly very massive with $M_* > 100M_\odot$ (e.g., Bromm, Coppi, & Larson 1999, 2002; Abel, Bryan, & Norman 2000, 2002; Nakamura & Umemura 2001; Bromm & Loeb 2004; Yoshida et al. 2006; Gao et al. 2007; O’Shea & Norman 2007). They had likely played a crucial role in driving early cosmic evolution by producing ionizing photons and heavy

elements. The initial stages in the reionization of the intergalactic medium (IGM) have recently been investigated in great detail with one and three dimensional simulations, showing the expansion of individual H II regions around the first stars (Kitayama et al. 2004; Whalen, Abel, & Norman 2004; Alvarez, Bromm, & Shapiro 2006; Johnson, Greif, & Bromm 2007). In addition, the first stars were responsible for the initial metal enrichment of the IGM, because the first supernova (SN) explosions rapidly dispersed the heavy elements that were produced during the short (several Myr) lifetime of Pop III stars into the environment. This process initiated the extended nucleosynthetic build-up of elements, starting from a hydrogen/helium mixture to a fully metal-rich gas (e.g., Madau, Ferrara, & Rees 2001; Mori, Ferrara, & Madau 2002; Scannapieco, Ferrara, & Madau 2002; Thacker, Scannapieco, & Davis 2002; Bromm, Yoshida, & Hernquist 2003; Furlanetto & Loeb 2003, 2005; Wada & Venkatesan 2003; Daigne et al. 2004, 2006a; Norman, O’Shea, & Paschos 2004; Yoshida, Bromm, & Hernquist 2004; Greif et al. 2007).

The early metal enrichment had important implications. In particular, the character of star formation changed from an early, high-mass dominated (Pop III) mode to the familiar, lower-mass (Pop II) mode, once a threshold level of enrichment had been reached, the so-called “*critical metallicity*”, $Z_{\text{crit}} \sim 10^{-3.5} Z_{\odot}$ (e.g., Omukai 2000; Bromm et al. 2001; Bromm & Loeb 2003a; Schneider et al. 2003, 2006; Frebel, Johnson, & Bromm 2007; Smith & Sigurdsson 2007). It is therefore important to explore the topology of early metal enrichment, and find when particular regions in the universe become supercritical (e.g., Schneider et al. 2002; Mackey, Bromm, & Hernquist 2003; Scannapieco, Schneider, & Ferrara 2003; Ricotti & Ostriker 2004; Furlanetto & Loeb 2005; Greif & Bromm 2006; Venkatesan 2006).

Gamma-Ray Bursts (GRBs) provide ideal probes of the formation rate and environmental impact of stars in the high-redshift universe, including the reionization and metal enrichment of the IGM. The high luminosities of GRBs make them detectable out to the edge of the visible universe (e.g., Lamb & Reichart 2000; Ciardi & Loeb 2000; Bromm & Loeb 2002; Naoz & Bromberg 2007). GRBs offer the exciting opportunity to detect the first (Pop III) stars, one star at a time. Although the detailed nature of the central engine that powers the relativistic jets of GRBs is still unknown, recent evidence indicates that GRBs trace the formation of massive stars (e.g., Totani 1997; Wijers et al. 1998; Blain & Natarajan 2000; Kulkarni et al. 2000; Porciani & Madau 2001; Bloom, Kulkarni, & Djorgovski 2002; Mesinger, Perna, & Haiman 2005; Natarajan et al. 2005; Daigne, Rossi, & Mochkovitch 2006b; but see Guetta & Piran 2007). There is growing

evidence that long-duration GRBs are associated with Type Ib/c SNe (e.g., Hjorth et al. 2003; Matheson et al. 2003; Stanek et al. 2003; see Woosley & Bloom 2006 for a recent review). The popular collapsar model for the central engine of long-duration GRBs (Woosley 1993; MacFadyen, Woosley, & Heger 2001 and references therein) involves the collapse of a massive star to a black hole (BH). Because of their high characteristic masses, a significant fraction of Pop III stars might end their lives as a BH, potentially leading to large numbers of high-redshift GRBs. In the hierarchical assembly process of halos which are dominated by cold dark matter (CDM), the first galaxies should have had lower masses (and lower stellar luminosities) than their low-redshift counterparts. Consequently, the characteristic luminosity of galaxies or quasars is expected to decline with increasing redshift. GRB afterglows, which already produce a peak flux comparable to that of quasars or starburst galaxies at $z \sim 1 - 2$, are therefore expected to outshine any competing source at the highest redshifts, when the first dwarf galaxies have formed in the universe (e.g. Ciardi & Loeb 2000; Gou et al. 2004; Inoue, Omukai, & Ciardi 2007).

The polarization data from the *Wilkinson Microwave Anisotropy Probe* (*WMAP*) indicates an optical depth to electron scattering of $\sim 9 \pm 3\%$ after cosmological recombination (Spergel et al. 2007). This implies that the first stars must have formed before a redshift $z \sim 10$, and reionized a substantial fraction of the intergalactic hydrogen by that time (e.g., Cen 2003; Ciardi, Ferrara, & White 2003; Somerville & Livio 2003; Wyithe & Loeb 2003; Yoshida et al. 2004). Early reionization can be achieved with plausible star formation parameters in the standard Λ CDM cosmology; in fact, the required optical depth can be achieved in a variety of very different ionization histories since *WMAP* places only an integral constraint on these histories (e.g., Haiman & Holder 2003; Greif & Bromm 2006). One would like to probe the full history of reionization in order to disentangle the properties and formation history of the stars that are responsible for it. GRB afterglows offer the opportunity to detect stars as well as to probe the ionization state (Barkana & Loeb 2004) and metal enrichment level (Furlanetto & Loeb 2003) of the intervening IGM out to redshifts $z > 10$. The detection of even a very small number of such high-redshift bursts could provide interesting constraints on the small-scale power spectrum of density fluctuations. Models with reduced small-scale power, such as warm dark matter (WDM) scenarios, could then be ruled out (Mesinger et al. 2005).

The potential high-redshift GRBs can be identified through infrared photometry, based on the Ly α break induced by absorption of their spectrum at wavelengths below $1.216 \mu\text{m} [(1+z)/10]$. Follow-up spectroscopy of high-

redshift candidates can then be performed on a 10-meter-class telescope. Recently, the ongoing *Swift* mission (Gehrels et al. 2004) has detected a GRB originating at $z \simeq 6.3$ (e.g., Haislip et al. 2006; Kawai et al. 2006), thus demonstrating the viability of GRBs as probes of the early universe.

There are four main advantages of GRBs relative to traditional cosmic sources such as quasars:

(i) The GRB afterglow flux at a given observed time lag after the γ -ray trigger is not expected to fade significantly with increasing redshift, since higher redshifts translate to earlier times in the source frame, during which the afterglow is intrinsically brighter (Ciardi & Loeb 2000). For standard afterglow lightcurves and spectra, the increase in the luminosity distance with redshift is compensated by this cosmological time-stretching effect. This is illustrated in Figure 15.1.

(ii) As already mentioned, in the standard Λ CDM cosmology, galaxies form hierarchically, starting from small masses and increasing their average mass with cosmic time. Hence, the characteristic mass of quasar black holes and the total stellar mass of a galaxy were smaller at higher redshifts, making these sources intrinsically fainter (Wyithe & Loeb 2002). However, GRBs are believed to originate from a stellar mass progenitor and so the intrinsic luminosity of their engine should not depend on the mass of their host galaxy. GRB afterglows are therefore expected to outshine their host galaxies by a factor that gets larger with increasing redshift.

(iii) Since the progenitors of GRBs are believed to be stellar, they likely originate in the most common star-forming galaxies at a given redshift rather than in the most massive host galaxies, as is the case for bright quasars (Barkana & Loeb 2004). Low-mass host galaxies induce only a weak ionization effect on the surrounding IGM and do not greatly perturb the Hubble flow around them (e.g., Alvarez et al. 2006; Johnson et al. 2007). Hence, the Ly α damping wing should be closer to the idealized unperturbed IGM case (Miralda-Escudé 1998) and its detailed spectral shape should be easier to interpret. Note also that unlike the case of a quasar, a GRB afterglow can itself ionize at most $\sim 4 \times 10^4 E_{51} M_{\odot}$ of hydrogen if its UV energy is E_{51} in units of 10^{51} ergs (based on the available number of ionizing photons), and so it should have a negligible cosmic effect on the surrounding IGM.

(iv) GRB afterglows have smooth (broken power-law) continuum spectra unlike quasars which show strong spectral features (such as broad emission lines or the so-called “blue bump”) that complicate the extraction of IGM absorption features. In particular, the continuum extrapolation into the Ly α damping wing (the Gunn-Peterson (1965) absorption trough) during the epoch of reionization is much more straightforward for the smooth UV

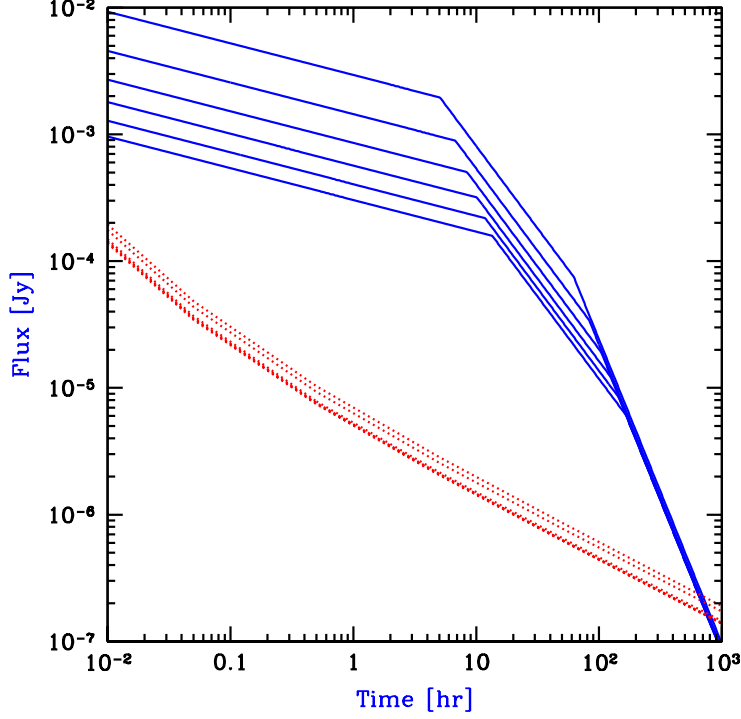


Fig. 15.1. Detectability of high-redshift GRB afterglows as a function of time since the GRB explosion as measured by the observer (adopted from Barkana & Loeb 2004). The GRB afterglow flux (in Jansky) is shown (*solid curves*) at the redshifted $\text{Ly}\alpha$ wavelength. Also shown (*dotted curves*) is the detection threshold for *JWST* assuming a spectral resolution $R = 5000$ with the near infrared spectrometer, a signal to noise ratio of 5 per spectral resolution element, and an exposure time equal to 20% of the time since the GRB explosion. In each set of curves, a sequence of redshifts is used, $z = 5, 7, 9, 11, 13, 15$, respectively (from top to bottom).

spectra of GRB afterglows than for quasars with an underlying broad $\text{Ly}\alpha$ emission line (Barkana & Loeb 2004).

In contrast to quasars of comparable brightness, GRB afterglows are short-lived and release ~ 10 orders of magnitude less energy into the surrounding IGM. Beyond the scale of their host galaxy, GRBs have a negligible effect on their cosmological environment. Note, however, that feedback from a single GRB or SN on the gas confined within early dwarf galaxies could be dramatic, since the binding energy of most galaxies at $z > 10$ is lower than 10^{51} ergs (Barkana & Loeb 2001). Consequently, GRBs are ideal probes of the IGM during the reionization epoch. Their rest-frame UV spectra can be

used to probe the ionization state of the IGM through the spectral shape of the Gunn-Peterson ($\text{Ly}\alpha$) absorption trough, or its metal enrichment history through the intersection of enriched bubbles of SN ejecta from early galaxies (Furlanetto & Loeb 2003). Afterglows that are unusually bright ($> 10\text{mJy}$) at radio frequencies could show a detectable forest of 21 cm absorption lines due to enhanced H I column densities in sheets, filaments, and collapsed minihalos within the IGM (Carilli, Gnedin, & Owen 2002; Furlanetto & Loeb 2002; but see Ioka & Mészáros 2005).

Another advantage of GRB afterglows is that once they fade away, one may search for their host galaxies. Hence, GRBs may serve as signposts of the earliest dwarf galaxies that are otherwise too faint or rare on their own for a dedicated search to find them. Detection of metal absorption lines from the host galaxy in the afterglow spectrum, offers an unusual opportunity to study the physical conditions (temperature, metallicity, ionization state, and kinematics) in the interstellar medium of these high-redshift galaxies. A small fraction ($\sim 10\%$) of the GRB afterglows are expected to originate at redshifts $z > 5$ (Bromm & Loeb 2002, 2006). As mentioned, this subset of afterglows can be selected photometrically using a small telescope, based on the $\text{Ly}\alpha$ break at a wavelength of $1.216\mu\text{m}[(1+z)/10]$, caused by intergalactic H I absorption. The challenge in the upcoming years will be to follow-up on these candidates spectroscopically, using a large (10-meter class) telescope.

GRB afterglows are likely to revolutionize observational cosmology and replace traditional sources like quasars, as probes of the IGM at $z > 5$. The near future promises to be exciting for GRB astronomy as well as for studies of the high-redshift universe. The *Swift* mission (Gehrels et al. 2004) has already greatly increased the number of GRBs with measured redshifts, with a mean redshift of $\langle z \rangle \sim 2$, compared to $\langle z \rangle \sim 1$ as estimated for the BATSE sample, including a few bursts detected at $z > 5$. Future missions, such as the planned EXIST satellite (Grindlay et al. 2006) which would provide synergy with the near-infrared follow-up capabilities of *JWST*, promise to further advance the emerging frontier of GRB cosmology.

Here, we will not discuss the possible use of GRBs as standard candles in probing the expansion history of the universe out to high redshifts, beyond what is currently possible with Type Ia SNe, to constrain cosmological parameters (e.g., see Schaefer 2003, 2007). Recently, the utility of GRBs as standard candles for cosmology has been seriously challenged (e.g., Butler et al. 2007; Li 2007), and it is currently not clear whether this methodology would provide a useful tool for precision cosmology. We will also not consider short-duration GRBs, as the associated timescale for the merger of

the binary compact-remnant progenitor is typically too long to probe cosmic evolution during the first hundreds of millions of years after the big bang.

This chapter is organized as follows. We begin by zooming in on the very small spatial scales around the GRB progenitor itself (Section 15.2), proceed to the intermediate scale of the GRB host system (Section 15.3), and finally consider the cosmological scale of the surrounding high- z IGM (Section 15.4). We conclude by discussing the utility of GRBs in probing the cosmic star formation history in the early universe (Section 15.5). This last section unifies all the different scales, with the ultimate goal of arriving at a coherent framework for understanding early cosmic star formation.

15.2 Population III GRB Progenitors

No GRB from a Pop III progenitor has been observed to date, but it is intriguing to ask: *What is the expected signature of GRBs that were triggered by the death of a massive Pop III star?* The information that a particular GRB originated at a high redshift is not sufficient to establish the case for the nature of its progenitor. For example, the currently highest-redshift GRB at $z \simeq 6.3$ (GRB 050904) clearly did not originate from a Pop III progenitor, given that the inferred level of metal enrichment in the host system is a few percent of the solar abundance (e.g., Campana et al. 2007). Pregalactic metal enrichment was inhomogeneous, and we expect normal Pop I and II stars to exist in galaxies that were already metal-enriched at these high redshifts. Pop III and Pop I/II star formation is thus predicted to have occurred concurrently at $z > 5$.

However, it is plausible that the high mass-scale for Pop III stars is reflected in the observational signature of the resulting GRBs. Specifically, we estimate that the mass of the BH at the center of the collapsar is a factor of 10 larger for Pop III, and the Pop III GRB distribution may thus be biased toward longer-duration events. It remains an open question as to what the exact dependence of the GRB duration, T_{dur} , is on the collapsar BH mass, but one might guess a simple linear relation to first order: $T_{\text{dur}} \propto R_{\text{Sch}}/c \propto M_{\text{BH}}$, where R_{Sch} is the Schwarzschild radius. The same linear scaling with mass might apply to the total energy released in γ rays, if one assumes that the energy yield is proportional to the total (rest mass) energy reservoir of the BH. The properties of the corresponding Pop III GRB afterglow emission are more uncertain (e.g., Ciardi & Loeb 2000; Gou et al. 2004; Inoue et al. 2007), because they depend sensitively on the circumburst density in the Pop III host system (see the next section).

Empirically, it is estimated that the ratio between the rates of intermediate-

redshift GRBs and core collapse SNe is $\sim 10^{-3}$ (e.g., Langer & Norman 2006). It is then important to estimate the corresponding GRB frequency for Pop III stars (e.g., Bromm & Loeb 2006). Conservatively, one could simply assume a constant efficiency of forming GRBs per unit mass of stars, independent of time and stellar population. Such an assumption, however, could be seriously in error. There are conflicting trends that could move the frequency of Pop III GRBs away from their low-redshift counterparts. Metal-free stars are predicted to have been massive (Abel et al. 2002; Bromm et al. 2002) and their extended envelopes may have suppressed the emergence of relativistic jets out of their surface (even if such jets were produced through the collapse of their core to a spinning black hole). On the other hand, low-metallicity stars are expected to have had weak winds with little angular momentum loss during their evolution, and so they may have preferentially produced rotating central configurations that make GRB jets after core collapse. *Should GRBs be a common phenomenon among the first metal-free stars?*

Long-duration GRBs appear to be associated with Type Ib/c supernovae (e.g., Stanek et al. 2003), namely progenitor massive stars that have lost their hydrogen envelope. The lack of an envelope was anticipated theoretically by the collapsar model, in which the relativistic jets produced by core collapse to a black hole are unable to emerge relativistically out of the stellar surface if the hydrogen envelope is retained (MacFadyen et al. 2001). The question then arises as to whether the lack of metal-line opacity that is essential for radiation-driven winds in metal-rich stars (e.g., Kudritzki & Puls 2000), would make a Pop III star retain its hydrogen envelope, thus quenching any relativistic jets and GRBs. There are, however, other mechanisms that might allow a Pop III star to shed its hydrogen envelope: (i) violent pulsations, particularly in the mass range $100\text{--}140M_{\odot}$, or (ii) a wind driven by helium lines. The outer atmospheres of these unusual stars are in a state where gravity only marginally exceeds radiation pressure due to electron-scattering (Thomson) opacity (e.g., Bromm, Kudritzki, & Loeb 2001). Adding the small, but still non-negligible contribution from the bound-free opacity provided by singly-ionized helium, may be able to unbind the atmospheric gas. Therefore, mass-loss could occur even in the absence of dust, or any heavy elements.

Assuming that long-duration GRBs are indeed produced by the collapsar mechanism, it is a matter of active debate whether a massive star with a close binary companion is the primary route to forming a GRB progenitor (rapidly spinning black hole) or whether single star progenitors are required (e.g., Petrovic et al. 2005). The former was suggested by Bromm & Loeb

(2006) for Pop III bursts to reconcile the two competing requirements of envelope removal in the absence of metal-line opacity and avoiding angular momentum loss. The same binary model was critically analysed by Belczynski et al. (2007), who argue that only a small fraction of possible close Pop III binaries will retain or acquire the spin required for the collapsar engine, when angular momentum transport is modelled with sufficient realism. It will be important, however, to explore more fully the complex physics of mass and angular momentum loss from Pop III stars, and to verify whether traditional stellar evolution models, such as those adopted by Belczynski et al. (2007), apply to metal-free stars. Interestingly, there has been suggestions for a single-star GRB progenitor that could circumvent some of the difficulties with realistic binary models (e.g., Yoon & Langer 2005; Woosley & Heger 2006; Yoon, Langer, & Norman 2006). The single-star models invoke stars that experience little mass loss and undergo chemically homogeneous nuclear burning, driven by rapid rotation. The star would then never leave the main sequence and expand into a red giant, so that a relativistic jet could pierce through the stellar material without being quenched. The requirement for reduced mass loss leads in turn to low metallicities ($< 0.1Z_{\odot}$) in the stellar atmospheres. Such a possible low-metallicity bias would be important in deriving the GRB redshift distribution from the cosmic star formation history (see §15.5).

15.3 Physical Properties of GRB Hosts

In order to predict the observational signature of high-redshift GRBs, we need to examine the unusual circumburst environment inside the systems that hosted the first stars. In particular, the properties of the afterglow emission that is associated with Pop III GRBs will sensitively depend on the density structure in the Pop III host system (e.g., Ciardi & Loeb 2000; Gou et al. 2004; Inoue et al. 2007). In general, higher densities translate to larger fluxes in the observer-frame near-infrared waveband, whereas the X-ray afterglows show almost no dependence on circumburst density (Gou et al. 2004).

What do we know about the host systems of Pop III star formation, and therefore of high-redshift GRBs? Within variants of the popular CDM model for structure formation, where small objects form first and subsequently merge to build up more massive ones, the first stars are predicted to form in the redshift range of $z \sim 20\text{--}30$ (Tegmark et al. 1997; Barkana & Loeb 2001; Yoshida et al. 2003). Figure 15.2 shows results from a cosmological simulation, illustrating the projected density field at $z = 20$. The bright

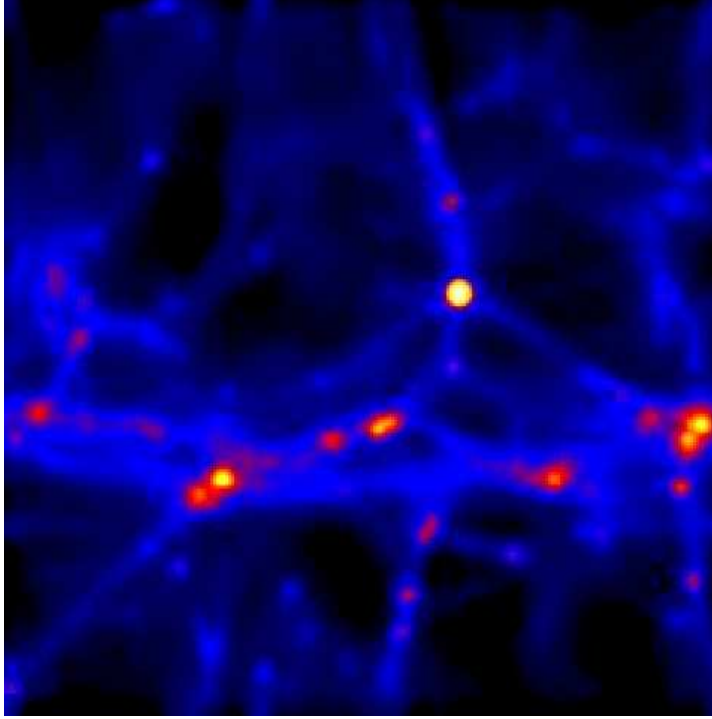


Fig. 15.2. Density field within a standard Λ CDM cosmology at $z = 20$. The box has a physical size of ~ 10 kpc. Shown is the projected gas density (with darker shades corresponding to lower density) which closely follows the dynamically dominant dark matter component. The bright knots at the intersection of the filamentary network are the sites where the first stars formed, and where the first GRBs might have exploded (from Bromm et al. 2003).

knots at the intersections of the filamentary network are so-called ‘minihalos’ of total mass (dark matter plus gas) $\sim 10^6 M_\odot$. These objects are the sites for the formation of the first stars, and thus are the potential hosts of the highest-redshift GRBs.

The identification of the environments in which potential Pop III GRBs and their afterglows occur, provides the motivation for studying the gas at the center of their host minihalos just before a massive star ends its life and the GRB explosion is triggered. This problem breaks down into two related questions: *(i)* what type of stars (in terms of mass, rotation, and clustering properties) will form in each minihalo?, and *(ii)* how will the ionizing radiation from each star modify the density structure of the surrounding gas? These two questions are fundamentally intertwined. The

production of ionizing photons depends strongly on the stellar mass, which in turn is determined by how the accretion flow onto the growing protostar proceeds under the influence of this radiation field. In other words, the assembly of the Pop III stars and the development of an H II region around them proceed simultaneously, and affect each other. The shallow potential wells in the host minihalos, with corresponding circular velocities of a few km s^{-1} , are unable to retain photo-ionized gas, so that the gas is effectively blown out of the minihalo. The resulting photo-evaporation has been studied with 3D radiative transfer calculations (e.g., Alvarez et al. 2006), where one massive Pop III star at the center of the minihalo acts as an embedded point source, that also take into account the hydrodynamic response of the photo-heated gas. It is possible to understand the key physics of the photo-evaporation from minihalos with the self-similar solution for a champagne flow (Shu et al. 2002). In Figure 15.3, we show the self-similar density evolution, scaled with parameters appropriate for the Pop III case. Note that the central density is significantly reduced by the end of the life of a massive star, and that a central core has developed in which the density is nearly constant. Such a flat density profile is markedly different from that created by stellar winds ($\rho \propto r^{-2}$). Winds, and consequently mass-loss, may not be important for massive Pop III stars (e.g., Baraffe, Heger, & Woosley 2001; Kudritzki 2002; but see 15.2), and such a flat density profile may be characteristic of GRBs that originate from metal-free Pop III progenitors.

The ultimate modeling goal is to carry out self-consistent simulations of the protostellar accretion process, taking account of the radiative feedback on its dynamics. The required coupled radiation hydrodynamics simulations are just beyond the cutting-edge of existing numerical capabilities. In the meantime, we can gain first insight by considering the results from a somewhat idealized 3D numerical simulation of the protostellar accretion flow inside a minihalo at $z \sim 20$ (Bromm & Loeb 2004). In this simulation, one high-density clump has formed at the center of the minihalo, possessing a gas mass of a few hundred solar masses. Soon after its formation, the clump becomes gravitationally unstable and undergoes runaway collapse. Once the gas has exceeded a threshold density of 10^7 cm^{-3} , a sink particle is inserted into the simulation. This choice for the density threshold ensures that the local Jeans mass is resolved throughout the simulation. The clump (i.e., sink particle) has an initial mass of $M_{\text{Cl}} \simeq 200 M_{\odot}$, and grows subsequently by ongoing accretion of surrounding gas. High-density clumps with such masses result from the chemistry and cooling rate of molecular hydrogen, H_2 , which imprint characteristic values of temperature, $T \sim 200 \text{ K}$, and density, $n \sim 10^4 \text{ cm}^{-3}$, into the metal-free gas (see

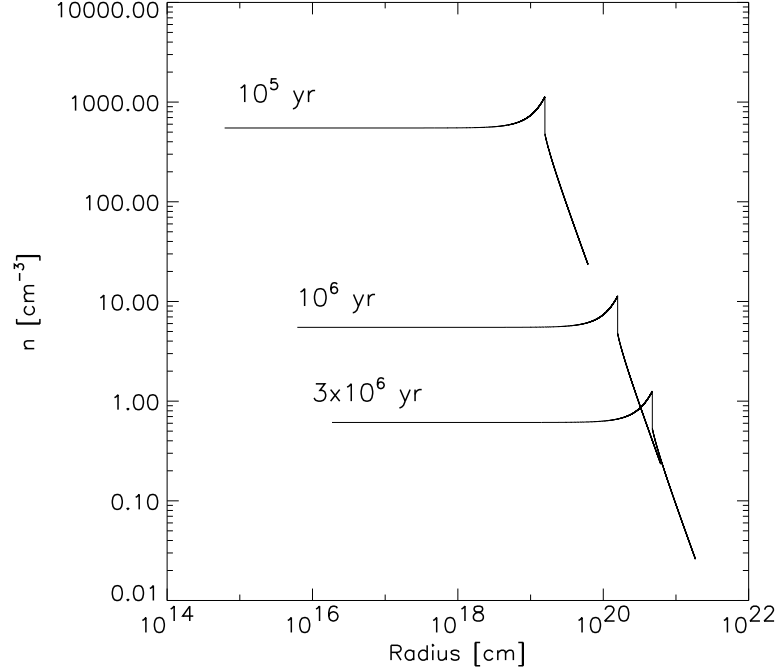


Fig. 15.3. Effect of photoheating from a Population III star on the density profile in a high-redshift minihalo. The curves, labeled by the time after the onset of the central point source, are calculated according to a self-similar model for the expansion of an H II region. Numerical simulations closely conform to this analytical behavior. Note that the central density is significantly reduced by the end of the life of a massive star, and that a central core has developed with a nearly constant density.

Bromm et al. 2002). Evaluating the Jeans mass for these characteristic values gives $M_J \sim \text{a few} \times 10^2 M_\odot$, which is close to the initial clump mass found in the simulation. The central clump is clearly not a star yet. To probe the subsequent fate of the clump, Bromm & Loeb (2004) have refined the resolution in the clump region to follow the collapse to higher densities (see Bromm & Loeb 2003b for a description of the refinement technique). The refined simulation allows one to study the three-dimensional accretion flow around the protostar (see also Omukai & Palla 2001, 2003; Ripamonti et al. 2002; Tan & McKee 2004). The gas now reaches densities of 10^{12} cm^{-3} before being incorporated into a central sink particle. At these high densities, three-body reactions (Palla, Salpeter, & Stahler 1983) have converted the gas into a fully molecular form. The growth of this molecular core is followed for the first $\sim 10^4$ yr after its formation, making the idealized as-

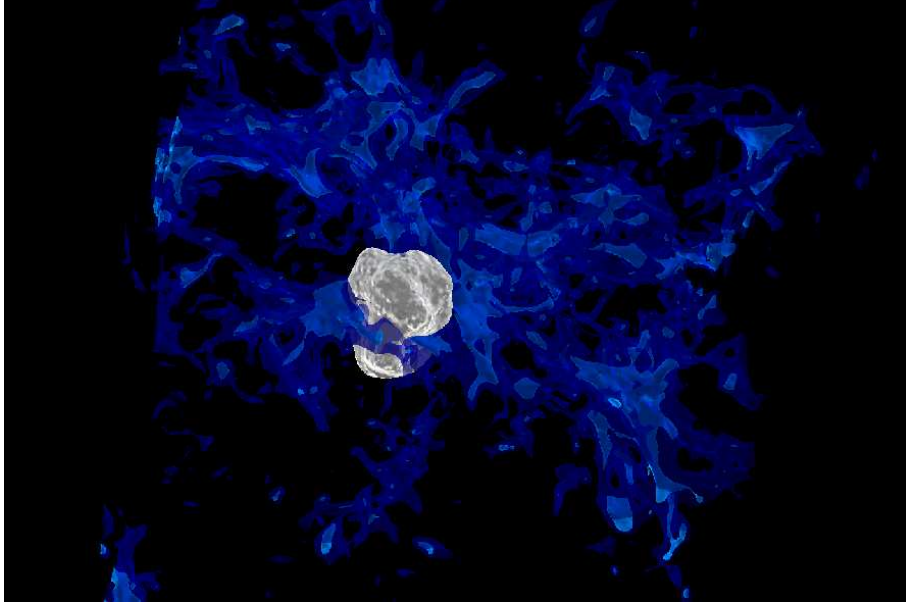


Fig. 15.4. Radiative feedback from the first stars (adopted from Johnson et al. 2007). The blue-dark contours show the density field at $z \sim 20$ within a cosmological box of physical size ~ 30 kpc. At the center of the box, a single Pop III star with $100M_{\odot}$ has formed, creating a bubble of ionized radiation (*white contour*) that reaches a maximum size of ~ 5 kpc (physical). The radiative feedback is fairly localized in extent, and leaves much of the surrounding IGM undisturbed. This snapshot shows the situation that would be present just before the Pop III star dies, possibly triggering a GRB explosion in the process. (Visualization courtesy of Paul Navrátil at the Texas Advanced Computing Center.)

sumption that the protostellar radiation does not affect the accretion flow. The accretion rate is initially very high, $\dot{M}_{\text{acc}} \sim 0.1M_{\odot} \text{ yr}^{-1}$, and subsequently declines roughly as a power law of time. The mass of the molecular core, taken as a crude estimate for the protostellar mass, grows with time t approximately as: $M_* \sim \int \dot{M}_{\text{acc}} dt \simeq 0.8M_{\odot} (t/1 \text{ yr})^{0.45}$. A robust upper limit for the final mass of the star is then: $M_*(t = 3 \times 10^6 \text{ yr}) \sim 500M_{\odot}$. In deriving this upper bound, we conservatively assumed that accretion cannot go on for longer than the total lifetime of a massive star of a few Myr. The numerical results can be understood within the general theoretical framework of how stars form (see Larson 2003). Star formation typically proceeds from the ‘inside-out’, through the accretion of gas onto a central hydrostatic core. Whereas the initial mass of the hydrostatic core is very similar for

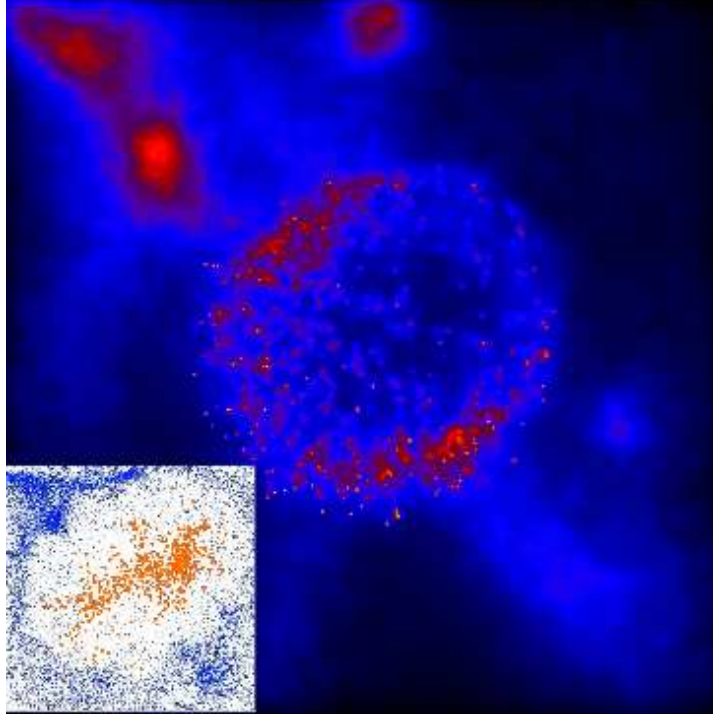


Fig. 15.5. Chemical feedback from the first stars (adopted from Bromm et al. 2003). SN explosion in the high-redshift universe that ends the life of a $200M_{\odot}$ Pop III star. The snapshot is taken $\sim 10^6$ yr after the explosion with total energy $E_{\text{SN}} \simeq 10^{53}$ ergs. We show the projected gas density within a box of linear size 1 kpc. The SN bubble has expanded to a radius of ~ 200 pc, having evacuated most of the gas in the minihalo. *Inset*: Distribution of metals. The stellar ejecta (*red dots*) trace the metals and are embedded in pristine metal-poor gas (*blue dots*).

primordial and present-day star formation (Omukai & Nishi 1998), the accretion process – ultimately responsible for setting the final stellar mass – is expected to be rather different. On dimensional grounds, the accretion rate is simply related to the sound speed (c_s) cubed over Newton’s constant (or equivalently given by the ratio of the Jeans mass and the free-fall time): $\dot{M}_{\text{acc}} \sim c_s^3/G \propto T^{3/2}$. A simple comparison of the temperatures in present-day star forming regions (with a temperature $T \sim 10$ K) with those in primordial ones ($T \sim 200 - 300$ K) already indicates a difference in the accretion rate of more than two orders of magnitude.

Can a Population III star ever reach this asymptotic mass limit? The answer to this question is not yet known with any certainty, and it depends on whether the accretion from a dust-free envelope is eventually terminated

by feedback from the star (e.g., Omukai & Palla 2001, 2003; Ripamonti et al. 2002; Omukai & Inutsuka 2002; Tan & McKee 2004). The standard mechanism by which accretion may be terminated in metal-rich gas, namely radiation pressure on dust grains (Wolfire & Cassinelli 1987), is obviously not effective for gas with a primordial composition. Recently, it has been speculated that accretion could instead be turned off through the formation of an H II region (Omukai & Inutsuka 2002), or through the radiation pressure exerted by trapped Ly α photons (Tan & McKee 2004). The termination of the accretion process defines the current unsolved frontier in studies of Pop III star formation. Understanding the GRB circumburst density structure at the highest redshifts requires further progress in the Pop III protostellar accretion problem.

The first galaxies may be surrounded by a shell of highly enriched material that was carried out in a SN-driven wind. A GRB in that galaxy may show strong absorption lines at a velocity separation associated with the wind velocity. Modelling these winds allows one to calculate the absorption profile in the featureless spectrum of a GRB afterglow. This will allow using the observed spectra of high- z GRBs to directly probe the degree of metal enrichment in the vicinity of the first star forming regions (see Furlanetto & Loeb 2003 for a semi-analytic treatment). As the early afterglow radiation propagates through the interstellar environment of the GRB, it will likely modify the gas properties close to the source; these changes could in turn be noticed as time-dependent spectral features in the spectrum of the afterglow and used to derive the properties of the gas cloud (density, metal abundance, and size). Perna & Loeb (1998) showed that the UV afterglow radiation can induce detectable changes to the interstellar absorption features of the host galaxy; Waxman & Draine (2000) and Fruchter, Krolik, & Rhoads (2001) examined the destruction of dust by the GRB X-rays, and Draine & Hao (2002) considered the destruction of molecules near the GRB source. Quantitatively, all of the effects mentioned above strongly depend on the exact properties of the gas in the host system.

15.4 Probing the High-Redshift IGM

The first stars transformed the early universe by ionizing the cosmic gas and enriching it with heavy elements that were not produced in the big bang. Understanding this cosmic metamorphosis is a key driver in modern cosmology. The goal is to complete the missing pages in our photo album of the universe which started at $z \sim 10^3$ when the universe became transparent and ended at the present epoch (Loeb 2006). Great progress has been made

so far in studying the emergence of cosmic structure with numerical simulations. In Figures 15.4 and 15.5, we show simulations of the radiative and chemical feedback from the first star to form in a cosmological simulation box. The radiative feedback represents the initial stage in the protracted process of reionization, whereas the chemical feedback is responsible for dispersing the first heavy elements into the chemically pristine IGM. Despite the importance for cosmology, we currently have only few and rather indirect observational constraints that would allow us to test our numerical and theoretical modelling of structure formation at high-redshift. GRBs offer the exciting prospect of directly probing the physical conditions in the IGM during the first billion years, when the first stars, galaxies and quasars emerged.

GRB afterglow emission at wavelengths close to the $\text{Ly}\alpha$ resonance could potentially provide a sensitive diagnostic of the ionization fraction in the IGM surrounding the explosion site (e.g., Miralda-Escudé 1998; Barkana & Loeb 2004). Specifically, the red damping wing with its reduced cross section for absorption compared to the line resonance allows to measure the IGM neutral fraction with high precision. In Figure 15.6, we show an illustrative example of this technique. High-resolution spectroscopy around the $\text{Ly}\alpha$ resonance in the afterglow spectrum of GRB 050904 at $z = 6.3$ (Totani et al. 2006) and of GRB 060927 at $z = 5.47$ (Ruiz-Velasco et al. 2007) revealed that the red damping wing is already saturated due to a large column density of neutral hydrogen in the host galaxy ($\log N_{\text{HI}} > 21.6 \text{ cm}^{-2}$), so that the spectra do not allow any inferences on the IGM neutral fraction at those redshifts. However, it is expected in hierarchical models of structure formation that the masses of star forming systems would decrease with increasing redshift, so that the neutral column densities will become smaller at higher z . In such a case, the damping wing will eventually reflect the conditions in the true IGM and not in the host systems.

In addition, high-redshift GRB afterglows also provide ideal ‘backlights’ to probe the IGM metal enrichment at different times. We illustrate this in Figure 15.7 (see Furlanetto & Loeb 2003 for additional details).

15.5 Cosmic Star Formation at High Redshifts

The cosmic star formation history at high redshifts is of great interest for our origins, since it started filling the universe with heavy elements such as carbon, oxygen or iron from which rocky planets and eventually living organisms are made. The star formation rate (SFR), together with possible variations in the stellar initial mass function (IMF), affect models of the

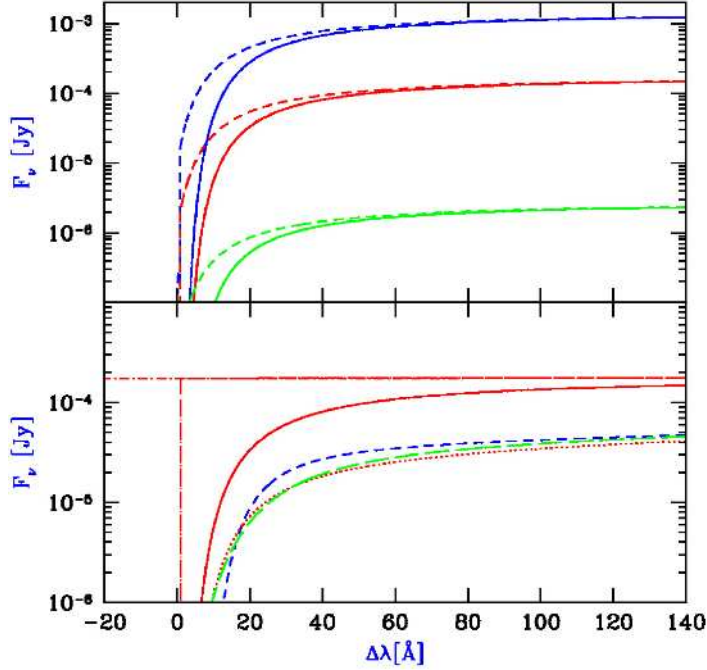


Fig. 15.6. Probing the ionization state of the IGM (from Barkana & Loeb 2004). IGM absorption profiles in GRB afterglows, presented in terms of the flux per unit frequency F_ν versus the observed wavelength shift from the $\text{Ly}\alpha$ resonance $\Delta\lambda$. *Top*: Predicted spectrum including H I absorption from the IGM (both resonant and damping wing), for host galaxies with source age 10^7 yr, an escape fraction of ionizing radiation $f_{\text{esc}} = 10\%$, and a normal IMF (*solid curves*) or a source age 10^8 yr, $f_{\text{esc}} = 90\%$, and a Pop III IMF (*dashed curves*). The observed time after the burst is (*top to bottom*) 1 h, 1 day, and 10 days. *Bottom*: Predicted spectra 1 day after a GRB for a host galaxy with a source age of 10^7 yr, $f_{\text{esc}} = 10\%$, and a normal IMF. Shown is the unabsorbed GRB afterglow (*dot-short-dashed curve*; essentially horizontal), the afterglow with resonant IGM absorption only (*dot-long-dashed curve*), and the afterglow with full (resonant and damping wing) IGM absorption (*solid curve*). Also shown, with 1.7 mag of extinction, are the afterglow with full IGM absorption (*dotted curve*) and attempts to fit this profile with a damped $\text{Ly}\alpha$ absorption system in the host galaxy (*dashed curves*).

initial stages of reionization (e.g., Wyithe & Loeb 2003; Ciardi, Ferrara, & White 2003; Sokasian et al. 2004; Yoshida et al. 2004; Greif & Bromm 2006; Johnson et al. 2007) and metal enrichment (e.g., Mackey et al. 2003; Furlanetto & Loeb 2003, 2005; Scannapieco et al. 2003; Schaye et al. 2003; Simcoe, Sargent, & Rauch 2004). Due to the inhomogeneous distribution of metals in the early universe, different modes of star formation occur si-

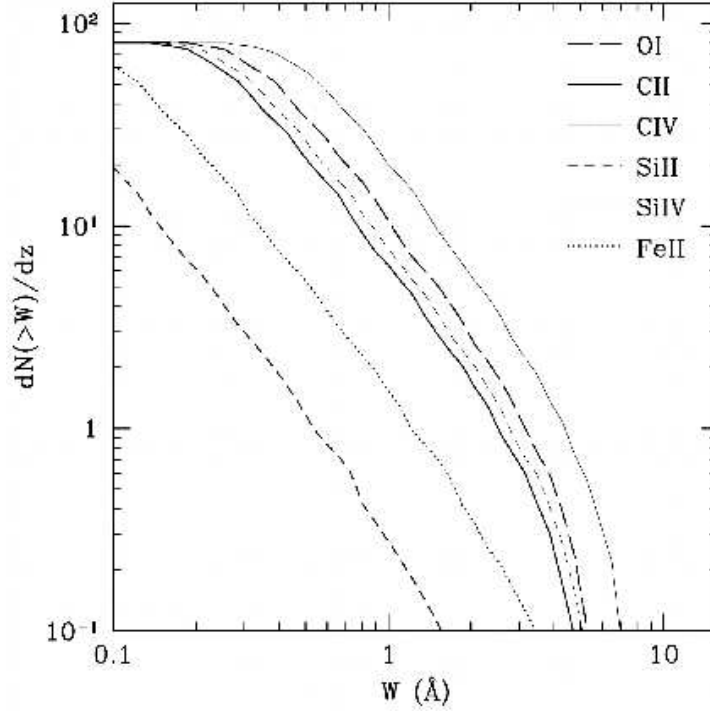


Fig. 15.7. Theoretical prediction for the feasibility probing the metal enrichment of the IGM at high redshifts (from Furlanetto & Loeb 2003). The different curves indicate the expected number of intersections by absorbers with an equivalent width above W (in Å) per unit redshift at $z = 8$, along the line-of-sight to a point source at a redshift $z > 8$. The different lines correspond to specific ionic species, as indicated in the figure.

multaneously: massive Pop III stars in regions of pristine gas, and normal mass Pop I/II stars in already enriched pockets. High- z GRBs will trace the overall cosmic SFR, regardless of whether the GRB progenitor belongs to Pop III or Pop I/II. Furthermore, it might be possible to separately probe Pop III star formation, provided that metal-free stars can trigger a GRB explosion with a signature that is clearly distinguished from the general population observed at lower redshifts (see Section 15.2). Constraints on the Pop III SFR from ongoing and future high- z GRB redshift surveys will be extremely valuable to determine whether planned missions, such as the *James Webb Space Telescope (JWST)*, will be able to effectively probe the first stars (e.g., Scannapieco et al. 2005). The constraints on Pop III star formation will also determine whether the first stars could have contributed a significant fraction to the cosmic near-IR background (e.g., Santos, Bromm,

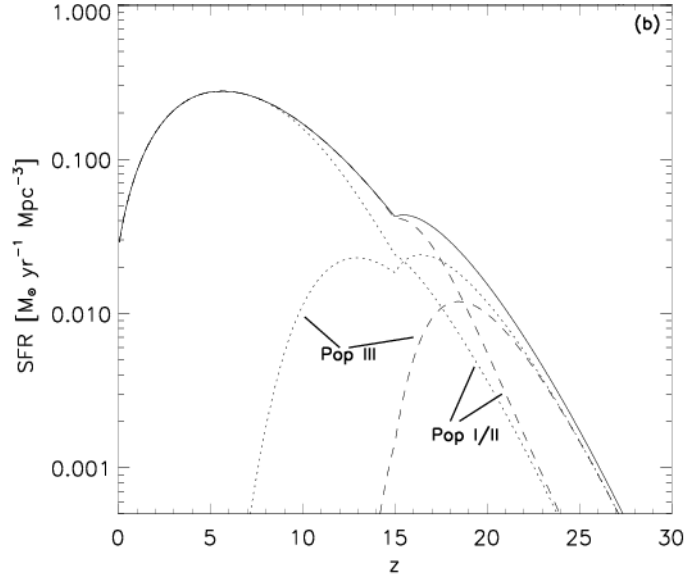


Fig. 15.8. Cosmic star formation rate (SFR) in units of $M_{\odot} \text{ yr}^{-1} (\text{comoving Mpc})^{-3}$, as a function of redshift (from Bromm & Loeb 2006). We assume that cooling in primordial gas is due to atomic hydrogen only, a star formation efficiency of $\eta_* = 10\%$, and reionization beginning at $z_{\text{reion}} \approx 17$. *Solid line*: Total comoving SFR. *Dotted lines*: Contribution to the total SFR from Pop I/II and Pop III for the case of weak chemical feedback. *Dashed lines*: Contribution to the total SFR from Pop I/II and Pop III for the case of strong chemical feedback. Pop III star formation is restricted to high redshifts, but extends over a significant range, $\Delta z \sim 10\text{--}15$.

& Kamionkowski 2002; Salvaterra & Ferrara 2003; Kashlinsky et al. 2005; Madau & Silk 2005; Dwek, Arendt, & Krennrich 2005).

Theoretical models of the high-redshift cosmic star formation history have a number of free parameters, such as the star formation efficiency and the strength of the chemical feedback. The latter refers to the timescale for, and spatial extent of, the distribution of the first heavy elements that were produced inside of Pop III stars and subsequently dispersed into the IGM by SN blast waves. From these SFRs, one can derive theoretical GRB redshift distributions, and one can then use the GRB redshift distribution observed by *Swift*, and any future missions such as EXIST, to calibrate the free model parameters. This technique could allow us to measure the redshift where Pop III star formation terminates, which in turn is a key ingredient in the modelling of reionization. In Figure 15.8 and 15.9, we illustrate this approach (based on Bromm & Loeb 2006). Figure 15.9 leads to the robust expectation that $\sim 10\%$ of all *Swift* bursts should originate at $z > 5$. This

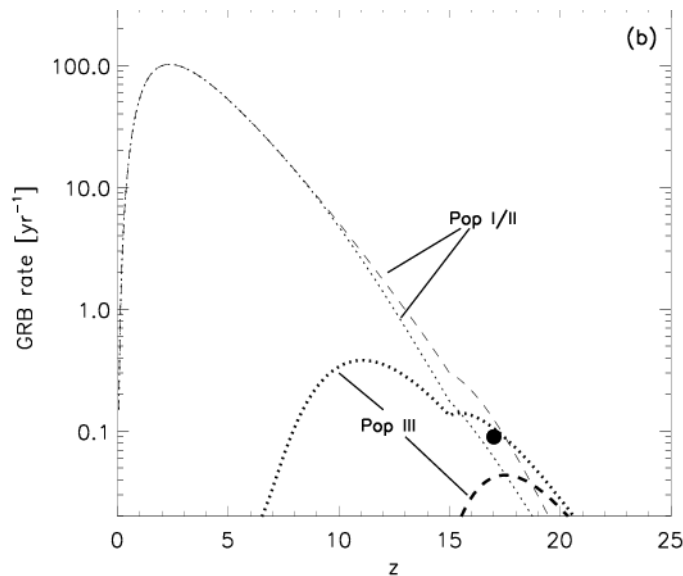


Fig. 15.9. Predicted GRB rate to be observed by *Swift* (from Bromm & Loeb 2006). Shown is the observed number of bursts per year, $dN_{\text{GRB}}^{\text{obs}}/d\ln(1+z)$, as a function of redshift. All rates are calculated with a constant GRB efficiency, $\eta_{\text{GRB}} \simeq 2 \times 10^{-9}$ bursts M_{\odot}^{-1} , using the cosmic SFRs from the previous figure. *Dotted lines*: Contribution to the observed GRB rate from Pop I/II and Pop III for the case of weak chemical feedback. *Dashed lines*: Contribution to the GRB rate from Pop I/II and Pop III for the case of strong chemical feedback. *Filled circle*: GRB rate from Pop III stars if these were responsible for reionizing the universe at $z \sim 17$.

prediction is based on the contribution from Population I/II stars which are known to exist even at these high redshifts. Additional GRBs could be triggered by Pop III stars, with a highly uncertain efficiency (see the discussion in 15.2).

A key ingredient in determining the underlying star formation history from the observed GRB redshift distribution is the GRB luminosity function, which is only poorly constrained at present. The improved statistics provided by *Swift* will enable the construction of an empirical luminosity function (see the preliminary studies by Salvaterra & Chincarini 2007; Guetta & Piran 2007). With an improved luminosity function and a better understanding of the observational selection effects for redshift measurements in GRB afterglows, one will be able to re-calibrate the theoretical prediction in Figure 15.9 more reliably.

Recent observations have indicated that long-duration GRBs preferentially originate in regions of low metallicity (Fruchter et al. 2006). The evidence is clear for low redshifts, $z < 0.25$, and low-luminosity GRBs (Stanek

et al. 2006). However, at higher redshifts and higher luminosities, the GRB environments appear to have metallicities that are somewhat *higher* than found in damped Ly α systems of similar hydrogen column densities (Savaglio, Fall, & Fiore 2003; Savaglio & Fall 2004; see Fig. 3 in Prochaska et al. 2007). Since stars are expected to form in the dense gaseous environments traced by damped Ly α at all redshifts, it appears that the progenitor stars of luminous GRBs do not originate preferentially in systems with exceedingly low-metallicities (for a recent review, see Savaglio 2006). The metallicity dependence of GRB progenitors has dramatic implications for the expected number counts of GRBs at high redshifts $z > 5$ (e.g., Salvaterra et al. 2007) and should be studied further.

Acknowledgements

We acknowledge support from NASA *Swift* grant NNX07AJ636.

References

- Abel, T., Bryan, G., & Norman, M. L. 2000, ApJ, 540, 39
- Abel, T., Bryan, G., & Norman, M. L. 2002, Science, 295, 93
- Alvarez, M. A., Bromm, V., & Shapiro, P. R. 2006, ApJ, 639, 621
- Baraffe, I., Heger, A., & Woosley, S. E. 2001, ApJ, 550, 890
- Barkana, R., & Loeb, A. 2001, Phys. Rep., 349, 125
- Barkana, R., & Loeb, A. 2004, ApJ, 601, 64
- Belczynski, K., Bulik, T., Heger, A., & Fryer, A. 2007, ApJ, in press (astro-ph/0610014)
- Blain, A. W., & Natarajan, P. 2000, MNRAS, 312, L35
- Bloom, J. S., Kulkarni, S. R., & Djorgovski, S. G. 2002, AJ, 123, 1111
- Bromm, V., Coppi, P. S., & Larson, R. B. 1999, ApJ, 527, L5
- Bromm, V., Coppi, P. S., & Larson, R. B. 2002, ApJ, 564, 23
- Bromm, V., Ferrara, A., Coppi, P. S., & Larson, R. B. 2001, MNRAS, 328, 969
- Bromm, V., Kudritzki, R. P., & Loeb, A. 2001, ApJ, 552, 464
- Bromm, V., & Larson, R. B. 2004, ARA&A, 42, 79
- Bromm, V., & Loeb, A. 2002, ApJ, 575, 111
- Bromm, V., & Loeb, A. 2003a, Nature, 425, 812
- Bromm, V., & Loeb, A. 2003b, ApJ, 596, 34
- Bromm, V., & Loeb, A. 2004, NewA, 9, 353
- Bromm, V., & Loeb, A. 2006, ApJ, 642, 382
- Bromm, V., Yoshida, N., & Hernquist, L. 2003, ApJ, 596, L135
- Butler, N. R., Kocevski, D., Bloom, J. S., & Curtis, J. L. 2007, ApJ, submitted (arXiv:0706.1275)
- Campana, S., et al. 2007, ApJ, 654, L17
- Carilli, C. L., Gnedin, N. Y., & Owen, F. 2002, ApJ, 577, 22
- Cen, R. 2003, ApJ, 591, L5
- Ciardi, B., Ferrara, A., & White, S.D.M. 2003, MNRAS, 344, L7
- Ciardi, B., & Ferrara, A. 2005, Space Sci. Rev., 116, 625
- Ciardi, B., & Loeb, A. 2000, ApJ, 540, 687

- Daigne, F., Olive, K. A., Silk, J., Stoehr, F., & Vangioni, E. 2006a, *ApJ*, 647, 773
- Daigne, F., Olive, K. A., Vangioni-Flam, E., Silk, J., & Audouze, J. 2004, *ApJ*, 617, 693
- Daigne, F., Rossi, E. M., & Mochkovitch, R. 2006b, *MNRAS*, 372, 1034
- Draine, B. T., & Hao, L. 2002, *ApJ*, 569, 780
- Dwek, E., Arendt, R. G., & Krennrich, F. 2005, *ApJ*, 635, 784
- Frebel, A., Johnson, J. L., & Bromm, V. 2007, *MNRAS*, in press (astro-ph/0701395)
- Fruchter, A., Krolik, J. H., & Rhoads, J. E. 2001, *ApJ*, 563, 597
- Fruchter, A., et al. 2006, *Nature*, 441, 463
- Furlanetto, S. R., & Loeb, A. 2002, *ApJ*, 579, 1
- Furlanetto, S. R., & Loeb, A. 2003, *ApJ*, 588, 18
- Furlanetto, S. R., & Loeb, A. 2005, *ApJ*, 634, 1
- Gao, L., Yoshida, N., Abel, T., Frenk, C. S., Jenkins, A., & Springel, V. 2007, *MNRAS*, in press (astro-ph/0610174)
- Gehrels, N., et al. 2004, *ApJ*, 611, 1005
- Gou, L. J., Mészáros, P., Abel, T., & Zhang, B. 2004, *ApJ*, 604, 508
- Greif, T. H., & Bromm, V. 2006, *MNRAS*, 373, 128
- Greif, T. H., Johnson, J. L., Bromm, V., & Klessen, R. S. 2007, *ApJ*, submitted (arXiv:0705.3048)
- Grindlay, J. E., et al. 2006, in *AIP Conf. Proc.* 836, *Gamma-ray Bursts in the Swift Era*, ed. S. S. Holt, N. Gehrels, & J. A. Nousek (Melville: AIP), 631
- Guetta, D., & Piran, T. 2007, *JCAP*, in press (arXiv:astro-ph/0701194)
- Gunn, J. E., & Peterson, B. A. 1965, *ApJ*, 142, 1633
- Haiman, Z., & Holder, G. P. 2003, *ApJ*, 595, 1
- Haislip, J., et al. 2006, *Nature*, 440, 181
- Heger, A., Fryer, C. L., Woosley, S. E., Langer, N., & Hartmann, D. H. 2003, *ApJ*, 591, 288
- Hjorth, J., et al. 2003, *Nature*, 423, 847
- Inoue, S., Omukai, K., & Ciardi, B. 2007, *MNRAS*, submitted (astro-ph/0502218)
- Ioka K., & Mészáros, P. 2005, *ApJ*, 619, 684
- Johnson, J. L., Greif, T. H., & Bromm, V. 2007, *ApJ*, in press (astro-ph/0612254)
- Kashlinsky, A., Arendt, R. G., Mather, J., & Moseley, S. H. 2005, *Nature*, 438, 45
- Kawai, N., et al. 2006, *Nature*, 440, 184
- Kitayama, T., Yoshida, N., Susa, H., & Umemura, M. 2004, *ApJ*, 613, 631
- Kitsionas, S., & Whitworth, A. P. 2002, *MNRAS*, 330, 129
- Kogut, A., et al. 2003, *ApJS*, 148, 161
- Kudritzki, R. P. 2002, *ApJ*, 577, 389
- Kudritzki, R. P., & Puls, J. 2000, *ARA&A*, 38, 613
- Kulkarni, S. R., et al. 2000, *Proc. SPIE*, 4005, 9
- Lamb, D. Q., & Reichart, D. E. 2000, *ApJ*, 536, 1
- Langer, N., & Norman, C. A. 2006, *ApJ*, 638, L63
- Larson, R. B. 2003, *Rep. Prog. Phys.*, 66, 1651
- Li, L.-X. 2007, *MNRAS*, in press (arXiv:0704.3128)
- Loeb, A. 2006, “First Light”, SAAS-Fee lecture notes, Springer, in press (astro-ph/0603360); see also Loeb, A. 2006, “The Dark Ages of the Universe”, *Scientific American*, 295, 46
- MacFadyen, A. I., Woosley, S. E., & Heger, A. 2001, *ApJ*, 550, 410
- Mackey, J., Bromm, V., & Hernquist, L. 2003, *ApJ*, 586, 1
- Madau, P., Ferrara, A., & Rees, M. J. 2001, *ApJ*, 555, 92
- Madau, P., & Silk, J. 2005, *MNRAS*, 359, L37

- Matheson, T., et al. 2003, *ApJ*, 599, 394
- Mesinger, A., Perna, R., & Haiman, Z. 2005, *ApJ*, 623, 1
- Miralda-Escudé, J. 1998, *ApJ*, 501, 15
- Miralda-Escudé, J. 2003, *Science*, 300, 1904
- Mori, M., Ferrara, A., & Madau, P. 2002, *ApJ*, 571, 40
- Nakamura, F., & Umemura, M. 2001, *ApJ*, 548, 19
- Naoz, S., & Bromberg, O. 2007, *MNRAS*, in press (astro-ph/0702357)
- Natarajan, P., Albanna, B., Hjorth, J., Ramirez-Ruiz, E., Tanvir, N., & Wijers, R. A. M. J. 2005, *MNRAS*, 364, L8
- Norman, M. L., O'Shea, B. W., & Paschos, P. 2004, *ApJ*, 601, L115
- Omukai, K. 2000, *ApJ*, 534, 809
- Omukai, K., & Inutsuka, S. 2002, *MNRAS*, 332, 59
- Omukai, K., & Nishi, R. 1998, *ApJ*, 508, 141
- Omukai, K., & Palla, F. 2001, *ApJ*, 561, L55
- Omukai, K., & Palla, F. 2003, *ApJ*, 589, 677
- O'Shea, B. W., & Norman, M. L. 2007, *ApJ*, 654, 66
- Palla, F., Salpeter, E. E., & Stahler, S. W. 1983, *ApJ*, 271, 632
- Perna, R., & Loeb, A. 1998, *ApJ*, 501, 467
- Petrovic, J., Langer, N., Yoon, S.-C., & Heger, A. 2005, *A&A*, 435, 247
- Porciani, C., & Madau, P. 2001, *ApJ*, 548, 522
- Prochaska, J. X., Chen, H.-W., Dessauges-Zavadsky, M., & Bloom, J. S. 2007, *ApJ*, submitted (astro-ph/0703665)
- Ricotti, M., & Ostriker, J. P. 2004, *MNRAS*, 350, 539
- Ripamonti, E., Haardt, F., Ferrara, A., & Colpi, M. 2002, *MNRAS*, 334, 401
- Ruiz-Velasco, A. E., et al. 2007, *ApJ*, submitted (arXiv:0706.1257)
- Salvaterra, R. S. Campana, S., Chincarini, G., Tagliaferri, G., & Covino, S. 2007, *MNRAS*, in press (arXiv:0706.0657)
- Salvaterra, R., & Chincarini, G. 2007, *ApJ*, 656, L49
- Salvaterra, R., & Ferrara, A. 2003, *MNRAS*, 339, 973
- Santos, M. R., Bromm, V., & Kamionkowski, M. 2002, *MNRAS*, 336, 1082
- Savaglio, S. 2006, *New J. Phys.*, 8, 195
- Savaglio, S., Fall, S. M., & Fiore, F. 2003, *ApJ*, 585, 638
- Savaglio, S., & Fall, S. M. 2004, *ApJ*, 614, 293
- Scannapieco, E., Ferrara, A., & Madau, P. 2002, *ApJ*, 574, 590
- Scannapieco, E., Madau, P., Woosley, S., Heger, A., & Ferrara, A. 2005, *ApJ*, 633, 1031
- Scannapieco, E., Schneider, R., & Ferrara, A., 2003, *ApJ*, 589, 35
- Schaefer, B. E. 2003, *ApJ*, 583, L67
- Schaefer, B. E. 2007, *ApJ*, 660, 16
- Schaye, J., Aguirre, A., Kim, T.-S., Theuns, T., Rauch, M., & Sargent, W. L. W. 2003, *ApJ*, 596, 768
- Schneider, R., Ferrara, A., Natarajan, P., & Omukai, K. 2002, *ApJ*, 571, 30
- Schneider, R., Ferrara, A., Salvaterra, R., Omukai, K., & Bromm, V. 2003, *Nature*, 422, 869
- Schneider, R., Salvaterra, R., Ferrara, A., & Ciardi, B. 2006, *MNRAS*, 369, 825
- Shu, F. H., Lizano, S., Galli, D., Cantó, J., & Laughlin, G. 2002, *ApJ*, 580, 969
- Simcoe, R. A., Sargent, W. L. W., & Rauch, M. 2004, *ApJ*, 606, 92
- Smith, B. D., & Sigurdsson, S. 2007, *ApJ*, 661, L5
- Sokasian, A., Yoshida, N., Abel, T., Hernquist, L., & Springel, V. 2004, *MNRAS*, 350, 47

- Somerville, R. S., & Livio, M. 2003, *ApJ*, 593, 611
Spergel, D. N., et al. 2007, *ApJS*, 170, 377
Springel, V., Yoshida, N., & White, S.D.M. 2001, *NewA*, 6, 79
Stanek, K. Z., et al. 2003, *ApJ*, 591, L17
Stanek, K. Z., et al. 2006, *Acta Astron.*, 56, 333
Tan, J. C., & McKee, C. F. 2004, *ApJ*, 603, 383
Tegmark, M., Silk, J., Rees, M. J., Blanchard, A., Abel, T., & Palla, F. 1997, *ApJ*, 474, 1
Thacker, R. J., Scannapieco, E., & Davis, M. 2002, *ApJ*, 581, 836
Totani, T. 1997, *ApJ*, 486, L71
Totani, T., et al. 2006, *PASJ*, 58, 485
Venkatesan, A. 2006, *ApJ*, 641, L81
Wada, K., & Venkatesan, A. 2003, *ApJ*, 591, 38
Waxman, E., & Draine, B. T. 2000, *ApJ*, 537, 796
Whalen, D., Abel, T., & Norman, M. L. 2004, *ApJ*, 610, 14
Wijers, R. A. M. J., Bloom, J. S., Bagla, J. S., & Natarajan, P. 1998, *MNRAS*, 294, L13
Wolfire, M. G., & Cassinelli, J. P. 1987, *ApJ*, 319, 850
Woosley, S. E. 1993, *ApJ*, 405, 273
Woosley, S. E., & Bloom, J. S. 2006, *ARA&A*, 44, 507
Woosley, S. E., & Heger, A. 2006, *ApJ*, 637, 914
Wyithe, J. S. B., & Loeb, A. 2002, *ApJ*, 581, 886
Wyithe, J. S. B., & Loeb, A. 2003, *ApJ*, 588, L69
Yoon, S.-C., & Langer, N. 2005, *A&A*, 443, 643
Yoon, S.-C., Langer, N., & Norman, C. A. 2006, *A&A*, 460, 199
Yoshida, N., Abel, T., Hernquist, L., & Sugiyama, N. 2003, *ApJ*, 592, 645
Yoshida, N., Bromm, V., & Hernquist, L. 2004, *ApJ*, 605, 579
Yoshida, N., Omukai, K., Hernquist, L., & Abel, T. 2006, *ApJ*, 652, 6